

# Anomalous Pull-Off Forces between Surfactant-Free Emulsion Drops in Different Aqueous Electrolytes

Hannah Lockie,<sup>†,§</sup> Rogerio Manica,<sup>‡</sup> Rico F. Tabor,<sup>†,§</sup> Geoffrey W. Stevens,<sup>†</sup> Franz Grieser,<sup>§</sup> Derek Y. C. Chan,<sup>||,⊥</sup> and Raymond R. Dagastine<sup>\*,†,‡,#</sup>

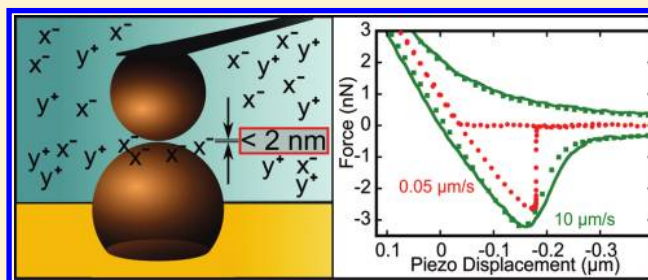
<sup>†</sup>Department of Chemical and Biomolecular Engineering and the Particulate Fluids Processing Centre, <sup>§</sup>School of Chemistry and the Particulate Fluids Processing Centre, and <sup>||</sup>Department of Mathematics and Statistics and the Particulate Fluids Processing Centre, The University of Melbourne, Parkville, VIC 3010, Australia

<sup>‡</sup>Institute of High Performance Computing, 1 Fusionopolis Way, 138632, Singapore

<sup>⊥</sup>Faculty of Life and Social Sciences, Swinburne University of Technology, Hawthorn, VIC 3122, Australia

<sup>#</sup>Melbourne Centre for Nanofabrication, 151, Wellington Road, Clayton, Victoria 3168, Australia

**ABSTRACT:** A systematic study of collisions between surfactant-free organic drops in aqueous electrolyte solutions reveals the threshold at which continuum models provide a complete description of thin-film interactions. For collision velocities above  $\sim 1 \mu\text{m/s}$ , continuum models of hydrodynamics and surface forces provide a complete description of the interaction, despite the absence of surfactant. This includes accurate prediction of coalescence at high salt concentration (500 mM). In electrolyte solutions at intermediate salt concentration (50 mM), drop–drop collisions at lower velocity ( $< 1 \mu\text{m/s}$ ) or extended time of forced drop–drop interaction exhibit a strong pull-off force of systematically varying magnitude. The observations have implications on the effects of ion-specificity and time-dependence in drop–drop interactions where kinetic stability is marginal.



## 1. INTRODUCTION

Understanding coalescence and kinetic stability in emulsion systems is important for a plethora of engineering applications.<sup>1</sup> Although it has been demonstrated experimentally that coalescence events are rapid,<sup>2</sup> the final stages of film drainage, and conditions that may act to prevent film rupture, are poorly understood. This is largely due to the difficulties in experimentally investigating films of thickness below 10 nm, particularly when the interfaces are free of stabilizing surfactants.

Previous atomic force microscope (AFM) work on drop–drop and bubble–bubble interactions have shown that the observed behavior can be accurately described by conventional physical models. By integrating hydrodynamics, surface forces, and shape changes during the interaction with the Stokes–Reynolds–Young–Laplace model, it has been demonstrated that continuum theories apply over almost the entire range of film thicknesses accessible in AFM force measurement systems.<sup>3–6</sup>

Observations of film structure and the dynamics of drainage in very thin films have led to the suggestion of deviations from continuum behavior. Several dynamic studies of films of water between rigid surfaces have indicated no water viscosity change from the bulk down to thin films of a few molecular layers,<sup>7–9</sup> whereas others have suggested that the effective viscosity may deviate from the continuum value at a separation less than 3

nm,<sup>10,11</sup> although this has proven difficult to quantify. Spectroscopic studies at both solid–liquid<sup>12</sup> and liquid–liquid<sup>13,14</sup> interfaces have suggested an increased regularity in water molecule orientation adjacent to the interface that may affect thin film behavior. In addition, the inadequacy of the point-charge description of ions in the Poisson–Boltzmann model or the presence of some other ion-specific effect has been suggested for a range of colloidal systems.<sup>15–17</sup>

Here, we use the AFM to investigate the behavior of aqueous films confined between alkane interfaces at electrolyte concentrations comparable to the onset of Hofmeister series effects in bulk systems.<sup>16</sup> Alkane drops of 50  $\mu\text{m}$  in radius have been used in the present study, giving molecularly smooth interfaces and kinetically stable thin films between drop pairs. Kinetic stability is due to the capacity of the drops for deformation and the negative charge at the interface, even in surfactant-free aqueous solutions.<sup>18–20</sup> Stability over a large interaction area and reduced roughness thus provide inherent consistency in results as compared to rougher, less stable, and more chemically varied solid systems. Furthermore, the weakness of the van der Waals attraction between oil drops in water, as compared to that between air bubbles,<sup>21</sup> and the

Received: December 2, 2011

Revised: January 29, 2012

Published: February 6, 2012

reduced interfacial tension, affords an additional stability, allowing access to thinner films ( $<7$  nm) where behavior may deviate from that of bubble films.

This study aims to offer some insight into the debate over the breakdown of continuum theories in relation to both aqueous film drainage and ion-specificity for deformable colloidal interactions. Identifying ion-specificity at chemically well-defined interfaces (such as the alkane–aqueous interface) will yield information regarding the solvated-ion environment that can be applied to more complex, often heterogeneously charged, interfaces in biological and engineering systems.

## 2. MATERIALS AND METHODS

**2.1. AFM Measurement.** An MFP3D Asylum Research (Santa Barbara, CA) AFM was used to measure the force between two alkane drops in aqueous solutions. The details of the measurement system and particular steps required to facilitate drop–drop measurements are detailed elsewhere.<sup>4,19</sup> First, a number of oil drops were stabilized on a hydrophobized, gold-coated, glass disk substrate. A drop was then picked up from the surface using a custom-made cantilever with a 45–65  $\mu\text{m}$  diameter hydrophobized gold disk patch at the free end.<sup>22</sup> The hydrophobicity of the gold-coated glass disk and the gold cantilever patch were tailored to facilitate drop transfer.<sup>19</sup>

Force measurements were performed between the drop positioned on the cantilever and a drop located on the gold-coated glass disk

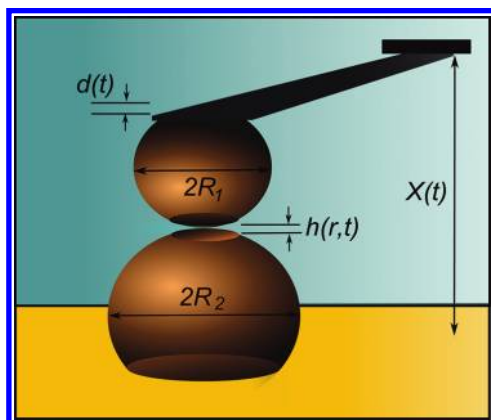


**Figure 1.** Schematic representation of the dynamic AFM force measurement system with drops immobilized on a gold-coated glass disk substrate, radius  $R_2$ , and a custom-made AFM cantilever with a gold patch area to which a drop, radius  $R_1$ , is anchored. Force is measured via cantilever deflection,  $d(t)$ , as a function of piezo travel,  $X(t)$ .

(illustrated in Figure 1). The force on the drop (positioned on a cantilever) was measured via the deflection ( $d(t)$ ) of the cantilever, monitored with an optical lever as the cantilever was driven toward and then away from the gold substrate at different velocities. The optical lever system was calibrated by measuring the deflection of the cantilever against a hard surface. The stiffness, or spring constant, of the cantilever was determined independently using the method described by Hutter et al.<sup>23</sup> For all measurements presented here, the spring constant measured and applied in force modeling was between 0.12 and 0.35 N/m. This technique allowed for the interaction forces between drops of 30–200  $\mu\text{m}$  radii to be measured at velocities of 0.02–100  $\mu\text{m/s}$ .

Distance of piezo travel as a function of time,  $X(t)$ , was measured directly for all force curves. Separation,  $h(r,t)$ , over the region of interaction of drops was extracted theoretically for deformable drop–drop interactions. The interfacial profile over the course of the interaction is calculated on the basis of coupling the hydrodynamic thin film drainage to the deformation of the drop. This is performed

through the normal pressure balance that accounts for surface forces disjoining pressure, drainage pressure, and deformation. Assumptions of viscosity and surface forces are made on the basis of established physical understanding, and the only fitted parameter in calculations is the initial separation,  $h(r,0)$ . Previous sensitivity studies of drop<sup>24</sup> and bubble<sup>3</sup> interactions have shown that the initial separation and drop profile can be determined to an accuracy of  $\pm 0.01$   $\mu\text{m}$ , equating to 0.1–1% error in the distance determination. This approach has been verified by independently measuring initial separation using a combined AFM–confocal microscopy technique.<sup>25</sup>

**2.2. Materials.** Tetradecane, hexadecane, and octyl acetate were obtained at  $>99\%$  (Sigma Aldrich) and column purified twice using Florosil 100–200 mesh (Sigma Aldrich). Salts of  $>99.9\%$  purity (Sigma Aldrich) were baked at 50  $^\circ\text{C}$  below their respective melting points for a minimum of 7 h to remove any organic contamination and used immediately. Solutions were prepared with Milli-Q purified water (resistivity of 18.2  $\text{M}\Omega$  cm). All glassware was carefully cleaned with Ajax soaking, nitric acid soaking, and thorough rinsing with Milli-Q purified water.

**2.3. Interfacial Tension.** Interfacial tension was obtained ex situ from the pendant drop geometry measured using a Dataphysics OCA 20 tensiometer. For all tetradecane drops in pure water, or aqueous electrolyte solutions of 2–100 mM concentration (with a range of monovalent salts), an interfacial tension of  $54 \pm 2$  mN/m was measured, indicating purity of the oil–water system. Changes in interfacial tension due to ion-type or concentration were not observed, possibly due to the limited precision of the measurement technique. The interfacial tension of tetradecane drops in electrolyte (50 mM  $\text{NaNO}_3$ ) solutions with 30% and 40% sucrose was measured as  $40 \pm 2$  and  $37 \pm 2$  mN/m, respectively, indicating some degree of interfacial activity of the sucrose species. Interfacial tensions of hexadecane and 3:1 mixtures of hexadecane and tetradecane showed no deviation from tetradecane interfacial tension (within experimental resolution), with values of  $54 \pm 2$  mN/m also measured in water and 50 mM  $\text{NaNO}_3$ , also indicating purity. Octyl acetate drops in water and a range of electrolyte solutions and concentrations ( $<50$  mM) were measured to have an interfacial tension of  $21 \pm 2$  mN/m.

## 3. RESULTS

**3.1. Hydrodynamic Interactions.** Drop–drop interactions with a collision velocity comparable to the rate of film drainage exhibit hydrodynamic forces, resulting in hysteresis between approach and retract branches of the force curve. On approach, hydrodynamic repulsion, in addition to surface forces, provides resistance to film drainage. On retract, an attractive force minimum is observed due to the limitation of the drainage rate as compared to the rate of the separation of the drops. A theoretical prediction of experimental forces of this nature is provided by the hydrodynamic theory of Chan et al.<sup>4,5</sup> This theory is applied here to model tetradecane drop–drop interactions in electrolyte solutions of several sodium salts at 50 mM concentration. It is shown in Figure 2 (with additional data and modeling in Figure 3a) that theory and experiment are well matched over a range of collision velocities comparable to Brownian motion velocities (1–15  $\mu\text{m/s}$ ).

Qualitatively, the behavior shown here at higher electrolyte concentrations (50 mM) is equivalent to drop–drop force measurements discussed in earlier work for both aqueous surfactant solutions<sup>4,19</sup> and surfactant-free aqueous solutions at low salt concentrations<sup>19</sup> (10 mM or less). However, at the higher salt concentration (50 mM) investigated here, an increase in the magnitude of the hydrodynamic forces is observed. This is due to the suppression of the electric double layer, allowing development of a very thin film ( $<10$  nm) during the interaction. The surface potentials needed to

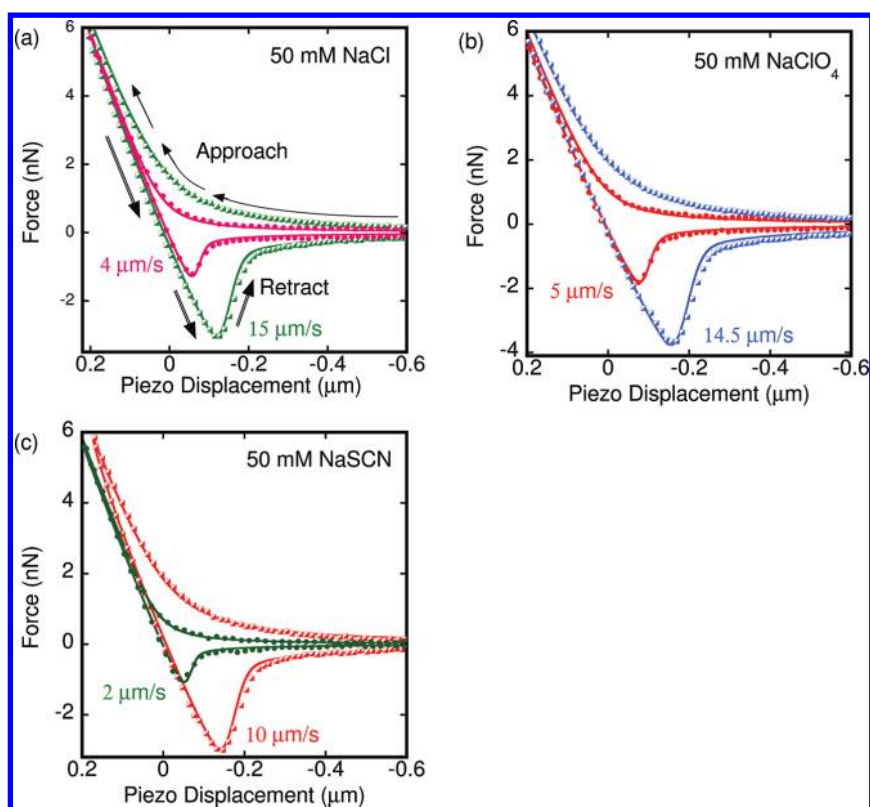


**Figure 2.** Experimental force (symbols) as a function of piezo displacement for a range of nominal velocities of collision (as indicated) between tetradecane drops of similar radii in 50 mM aqueous solutions of (a) NaCl at 15  $\mu\text{m/s}$  ( $\blacksquare$ ) and 4  $\mu\text{m/s}$  ( $\bullet$ ) with approach (single line) and retract (double line) branches of force curve indicated; (b) NaClO<sub>4</sub> at 14.5  $\mu\text{m/s}$  ( $\blacksquare$ ) and 5  $\mu\text{m/s}$  ( $\bullet$ ); and (c) NaSCN at 10  $\mu\text{m/s}$  ( $\blacksquare$ ) and 2  $\mu\text{m/s}$  ( $\bullet$ ) matched to predictions of the Stokes–Reynolds–Young–Laplace model (lines).<sup>5</sup> A surface potential of  $-20$  mV and Hamaker constant of  $5 \times 10^{-21}$  J are used in all cases for theoretical modeling.

produce the theoretical results in Figure 2 are independent of electrolyte type.

**3.2. Quasi-Static Interactions.** Comparison of the interaction between the same pair of drops under dynamic ( $>1$   $\mu\text{m/s}$  collision velocity) and quasi-static ( $<1$   $\mu\text{m/s}$  collision velocity) collision velocities in a 50 mM NaNO<sub>3</sub> aqueous solution is provided in Figure 3. At 10 and 1  $\mu\text{m/s}$ , the results are in excellent agreement with theory (Figure 3a). At slower nominal velocities (0.05–0.2  $\mu\text{m/s}$ ), the approach portions of the force curves overlap (Figure 3b), indicative of a negligible hydrodynamic contribution to the force. Upon retraction, the interactions at slow velocities show a deep attractive minimum followed by a sharp pull-off force. This is clearly distinguishable from the smooth hydrodynamic retraction minimum force at faster velocities (Figure 3a), the depth of which increases with increasing velocity. In contrast, the depth of the slow-velocity pull-off minimum increases with decreasing velocity (Figure 3b). Such a minimum in the retract branch of the force curve is observed consistently between concentrations of 20 and 100 mM for all monovalent salts investigated, showing an anion dependency, as discussed later. It was found that Cs<sup>+</sup> and K<sup>+</sup> electrolyte solutions provided approximately equivalent interactions to Na<sup>+</sup> electrolytes at equivalent concentration (with the same anion), indicating that there is no cation dependency.

The magnitude of the minimum prior to the pull-off force can be increased through varying the velocity of collision or the extent to which the drops are pushed together. This is demonstrated in Figure 4 for slow collision velocity interactions between drops in 50 mM NaSCN solution. An increase in the depth of the minimum is observed when the collision velocity is

reduced from 0.3 to 0.1  $\mu\text{m/s}$ , with extension to approximately the same maximum force. A similar increase is also observed for the two force measurements at 0.1  $\mu\text{m/s}$ , with a deeper minimum resulting from a higher maximum force attained during the interaction. This shows that the force minimum prior to pull-off may be dependent not only on the velocity of the interaction, but also on the duration of the interaction or the maximum interfacial area of interaction attained. Indeed, the depth of the minimum for a range of slow collisions is found to scale approximately with the square root of the time of the interaction, where this is defined as the point at which drops first interact (the cantilever deflects indicating a nonzero force), and the point at which drops “pull-off”. An example of these points is circled in Figure 4.

**3.3. Surface Forces Theory.** There is negligible difference in force as a function of piezo displacement during approach over the slow velocity range in aqueous solutions of 50 mM NaNO<sub>3</sub> (Figure 3) and NaSCN (Figure 4), indicating that hydrodynamic pressure is negligible, and the interaction might be well described by the static force theory of Chan, Dagastine, and White.<sup>26–28</sup> This analytical theory calculates deformation of drops over both the interacting film and the outer drop, and forces during the interaction as a function of drop–drop separation, and subsequently AFM piezo displacement. Key model inputs are drop size, interfacial tension, and disjoining pressure over the range of interface separations. Analysis has been performed to assess whether existing surface forces models for oil drops in pure electrolyte interactions can account for the observed approach and retract behavior.

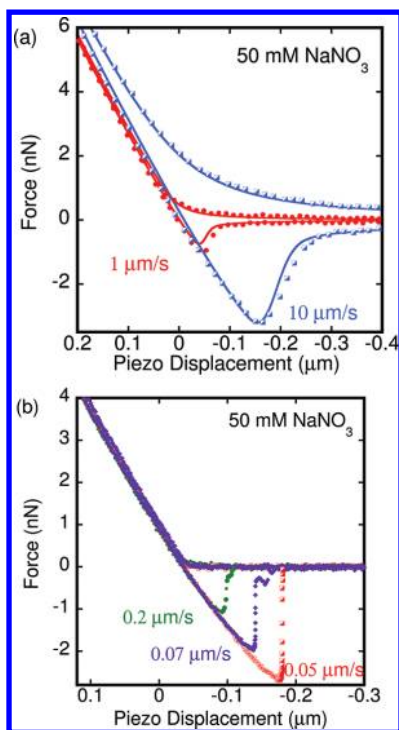


**Figure 3.** (a) Experimental (symbols) force as a function of piezo displacement matched to predictions of the Stokes–Reynolds–Young–Laplace model (lines) for interactions between tetradecane drops of 70 and 43  $\mu\text{m}$  radii in aqueous solution of 50 mM  $\text{NaNO}_3$  at collision velocities of 1  $\mu\text{m}/\text{s}$  ( $\bullet$ ) and 10  $\mu\text{m}/\text{s}$  ( $\blacksquare$ ). (b) Force as a function of piezo displacement for equivalent drops and solution as in (a) showing pull-off interaction upon retract at collision velocities of 0.05  $\mu\text{m}/\text{s}$  ( $\blacksquare$ ), 0.07  $\mu\text{m}/\text{s}$  ( $\blacklozenge$ ), and 0.2  $\mu\text{m}/\text{s}$  ( $\bullet$ ). For ease of viewing, 0.5–1% of data points are displayed.

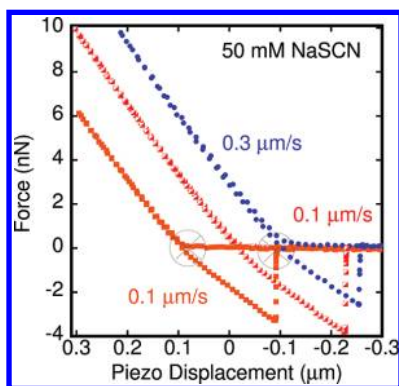


**Figure 4.** Force as a function of piezo displacement for interactions between tetradecane drops of 70 and 43  $\mu\text{m}$  radii in an aqueous solution of 50 mM  $\text{NaSCN}$  showing interactions to  $\sim 10$  nN force at collision velocities of 0.1  $\mu\text{m}/\text{s}$  ( $\blacksquare$ ) and 0.3  $\mu\text{m}/\text{s}$  ( $\bullet$ ), and a collision to 6 nN at 0.1  $\mu\text{m}/\text{s}$  ( $\blacksquare$ ). Start and end points of the “time of interaction” are indicated with circled crosses. For ease of viewing, 0.5–1% of data points are displayed, and curves are offset.

Electric double layer and van der Waals forces (a DLVO model) were used to construct a disjoining pressure<sup>29</sup> as a function of separation for a 50 mM 1:1 electrolyte between planar tetradecane interfaces using a surface potential of  $-14$  mV. This surface potential is the lowest possible value that will result in stable drop interactions for drops of the Laplace pressure of those presented in Figures 3b and 4. The resulting model calculation of the force–piezo displacement curve is

illustrated in Figure 5. This profile is a direct result of the secondary minimum in the disjoining pressure (shown in the

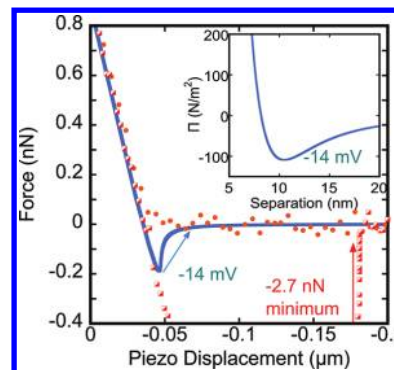


**Figure 5.** Experimental (symbols) force as a function of piezo displacement for interactions between tetradecane drops 70 and 43  $\mu\text{m}$  radii in an aqueous solution of 50 mM  $\text{NaNO}_3$  with a collision velocity of 0.05  $\mu\text{m}/\text{s}$  on approach ( $\bullet$ ) and retract ( $\blacksquare$ ). Theoretical (blue line) force as a function of piezo displacement for experimental drops under assumption of a DLVO disjoining pressure with a constant surface potential of  $-14$  mV with retarded van der Waals force, illustrating small pull-off prediction. (Inset) Disjoining pressure as a function of separation for flat tetradecane interfaces in solution of 50 mM 1:1 electrolyte assuming DLVO behavior with a surface potential  $-14$  mV with retarded van der Waals forces illustrating a secondary minimum.

inset of Figure 5) and can generate a hysteresis in the force–piezo displacement curve, as demonstrated by others,<sup>30,31</sup> and denoted here by the arrow in Figure 5. Although this secondary minimum can generate a hysteresis and a “jump-out” in the force–displacement curve, the attractive force minimum on retraction is too shallow by a factor of 10. Thus, we conclude that the deep pull-off force observed experimentally cannot be accounted for by DLVO interactions.

In addition to significantly underestimating the magnitude of the attractive minimum upon retract, there are two more indications that the DLVO description is not accurate. First, as highlighted above, the slow-velocity approach curves overlap for a range of velocities (0.05–0.3  $\mu\text{m}/\text{s}$ ), but the hysteresis observed on retract varies significantly with velocity. This cannot be explained with static DLVO surface forces theory. Second, in no case does a “jump-in” occur experimentally on approach. This should occur theoretically in conjunction with the jump-out for cases where continuum drainage and surface forces provide an accurate description of the collision.<sup>30,31</sup> For example, in Figure 5 for the case of  $-14$  mV, a jump-in would be expected at a relative piezo displacement of  $\sim 0.055$   $\mu\text{m}$ . However, experimental measurement of drop–drop approach shows a monotonically increasing positive (repulsive) force.

As noted in section 3.1, there are uncertainties associated with DLVO surface force contributions to the interaction, with the possibility that non-DLVO contributions are also important, particularly at short-range. The results of Figure 5 demonstrate that reasonable DLVO forces cannot describe the measured interaction even when allowing for uncertainties in surface forces parameters (e.g., error in surface-potential or van der Waals force calculations). In addition, assessment of a range of non-DLVO contributions found that, based on existing models of colloidal surface forces in noncontacting systems, including steric forces and depletion attractions, no reasonable

addition could produce a theoretical prediction equivalent to the attraction and subsequent pull-off observed experimentally.

**3.4. Ion-Specificity.** Interaction forces at a nominal velocity of  $0.2 \mu\text{m/s}$  are shown in Figure 6a with no measurable

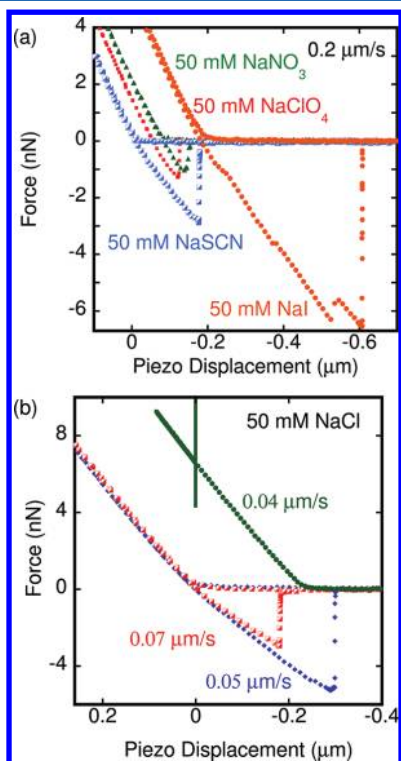


**Figure 6.** (a) Force as a function of piezo displacement for interactions between tetradecane drops of reduced radii  $50\text{--}53 \mu\text{m}$  radii in aqueous solutions of  $50 \text{ mM NaI}$  ( $\bullet$ ),  $50 \text{ mM NaSCN}$  ( $\blacksquare$ ),  $50 \text{ mM NaClO}_4$  ( $\blacksquare$ ), and  $50 \text{ mM NaNO}_3$  ( $\blacktriangle$ ) at a velocity of  $0.2 \mu\text{m/s}$ . (b) Force as a function of piezo displacement for interactions between drops of reduced radius  $51 \mu\text{m}$  in  $50 \text{ mM NaCl}$  aqueous solutions at velocities of  $0.7 \mu\text{m/s}$  ( $\blacklozenge$ ),  $0.5 \mu\text{m/s}$  ( $\blacksquare$ ), and  $0.4 \mu\text{m/s}$  ( $\bullet$ , with coalescence on retract). For ease of viewing, 0.5–1% of data points are displayed, and curves are offset in both plots.

difference on approach for the 1:1 sodium salts investigated. However, for a range of anion types, there are significant differences in the retract branches of the force curves. The magnitude of the pull-off force minimum increases significantly from  $\text{NO}_3^-$  to  $\text{ClO}_4^-$  to  $\text{SCN}^-$  to  $\text{I}^-$ . Measurements were taken with the same drops of approximately equal size, to within  $\pm 2 \mu\text{m}$  in terms of the reduced radius,  $R_{\text{reduced}}$  ( $2/R_{\text{reduced}} = 1/R_1 + 1/R_2$ ) with the same cantilever. Because all physical and experimental parameters, apart from the ion type, are comparable for the force curves presented in Figure 6a, this suggests that the observed variations in pull-off minima can be attributed to ion-specificity.

Tetradecane drop interactions in  $50 \text{ mM NaCl}$  aqueous solution are illustrated in Figure 6b at nominal velocities of  $0.4\text{--}0.7 \mu\text{m/s}$ , with approximately equivalent sized drops as those used in Figure 6a. Drop coalescence occurred during the retraction branch of the  $0.4 \mu\text{m/s}$  force curve. Hence, in contrast to other sodium salts, no measurements could be made at a collision velocity of  $0.2 \mu\text{m/s}$ . This suggests that for  $\text{NaCl}$  the stabilizing effect observed with the other salts is not sufficient to prevent van der Waals attraction dominating, resulting in coalescence. In addition, the depth of the minimum

observed at a collision velocity of  $0.5 \mu\text{m/s}$  is significantly greater for the  $\text{Cl}^-$  system, than in the case of  $\text{SCN}^-$ ,  $\text{NO}_3^-$ , or  $\text{ClO}_4^-$  at a slower velocity. A decrease in film stability (triggering coalescence) in systems with an increase in the pull-off minimum suggests, as logically expected, that the depth of the minimum may be enhanced by a decrease in film thickness.

It is observed that the pull-off in the  $\text{NaI}$  system shows a “double-jump” behavior. The double pull-off occurs frequently in systems where the minimum prior to pull-off is large. With a pull-off minimum of  $-7 \text{ nN}$ , as measured for the  $\text{NaI}$  curve in Figure 6a, the occurrence of a double jump is common. The origin of this effect is unclear and not precisely reproducible. Given the effect shows small variations within equivalent interactions, it may be due to nonaxisymmetric drainage, increasing where the attractive force holding drops at close separation is increased. Alternatively, it may be due to strong magnitude attractions experiencing two stages of rapid dynamic drainage with an outer-rim pull-off followed by an inner-film pull-off. These possibilities are speculative at this stage.

Ion-specificity can be investigated through a solution exchange method,<sup>32</sup> with changes in the magnitude of the pull-off force during drop–drop interactions observed. For example, the sequence  $\text{NaCl}$  to  $\text{NaNO}_3$  produces a consistent increase in the depth of the pull-off minimum; however, the reverse sequence does not provide the same result. This is possibly due to  $\text{NO}_3^-$  ions having greater affinity for adsorption to the oil–water interface than  $\text{Cl}^-$  and a kinetically limited desorption rate. This allows the  $\text{NO}_3^-$  behavior to dominate once its bulk solution is passed once through the fluid cell, and effectively reduces the presence of  $\text{Cl}^-$  in the confined film from that which would be present in the initial  $\text{NaCl}$  system. This hypothesis is supported by vibrational sum frequency spectroscopy (VSFS) that shows a greater interfacial affinity of  $\text{NO}_3^-$  as compared to  $\text{Cl}^-$ .<sup>14,33</sup> Given the complexity of preferential ion-presence at the interface,<sup>34</sup> and the fact that this does not provide data suitable for direct comparison of ionic species, analysis of path dependence through solution exchange is not presented here.

Figure 7 illustrates behavior as the concentration of  $\text{NaNO}_3$  is increased from  $50$  to  $500 \text{ mM}$ . At the higher concentration, the electric double layer forces are not present, and, when hydrodynamic drainage forces during drop collision are insufficient to maintain the film between the drops, their interfaces approach to a sufficiently small separation on retract for van der Waals forces to dominate, driving coalescence. For the drop-pair of Figure 7, it is shown that this occurs with a reduction in approach velocity from  $30$  to  $20 \mu\text{m/s}$ . Theoretical modeling of the interaction is well matched to the experimental observations, including close prediction of the point of coalescence in the  $20 \mu\text{m/s}$  interaction. Coalescence on retract may initially appear counterintuitive; however, this has been observed in microfluidic drop systems,<sup>35</sup> AFM bubble experiments,<sup>3</sup> and is explained theoretically<sup>3,36</sup> by the additional attractive hydrodynamic pressure that arises upon retract driving the drops closer together than the minimum thickness achieved on approach. The observation of coalescence at  $20 \mu\text{m/s}$  but not at  $30 \mu\text{m/s}$  illustrates that the variation in film thickness determined by the balance of deformation, hydrodynamic drainage surface forces, and the rate of separation is a complex process.

The modeling in Figure 7 predicts film thinning to approximately  $2 \text{ nm}$ , where thinner films are not stable due

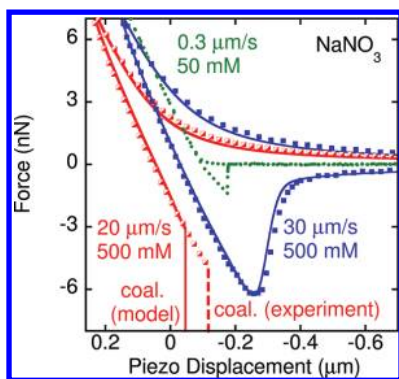


**Figure 7.** Experimental (symbols) force as a function of piezo displacement for interactions between tetradecane drops of 57 and 37  $\mu\text{m}$  radii in an aqueous solution of 50 mM  $\text{NaNO}_3$  at a collision velocity of 0.3  $\mu\text{m/s}$  ( $\bullet$ ), and in 500 mM  $\text{NaNO}_3$  at 30  $\mu\text{m/s}$  ( $\blacksquare$ ) and 20  $\mu\text{m/s}$  ( $\blacktriangle$ ). Hydrodynamic force curves at 500 mM are matched to predictions of the Stokes–Reynolds–Young–Laplace model (lines).<sup>5</sup> Coalescence is observed experimentally (dotted line) and predicted theoretically (solid line) at 20  $\mu\text{m/s}$ . A surface potential of  $-19$  mV and Hamaker constant of  $5 \times 10^{-21}$  J are required for theoretical modeling.

to the strength of the van der Waals force. In addition, a sensitivity study found that the stability of collisions is highly dependent on small changes to surface potential, with matching of experimental and theoretical results only at a surface potential of  $-19$  mV for the 500 mM system. An increase to  $-18$  mV produced incorrect coalescence predictions, and a decrease to  $-20$  mV produced an insufficient minimum force, resulting in stable collisions. Coalescence at concentrations of 500 mM is observed with all sodium salts at slow velocities, highlighting the lack of ion-steric inhibition to coalescence at high concentrations.

Complete modeling of the interactions at fast velocities of collision, where very thin films ( $\sim 2$  nm) are formed, indicates that the limitations on modeling the interaction at slower velocities of collision where the pull-off is observed are not associated simply with the thickness of the film attained.

**3.5. Viscosity Dependence.** Previous studies have shown that the addition of sucrose to an aqueous surfactant system results in an increase in the depth of the attractive hydrodynamic minimum between a large solid probe and an oil drop, consistent with the Stokes–Reynolds–Young–Laplace model using the appropriate bulk viscosity.<sup>24</sup> The effects of increasing the viscosity of the bulk solution through addition of sucrose to the 50 mM  $\text{NaNO}_3$  aqueous solution are shown in Figure 8a, revealing a similar anomalous behavior as seen with the nonsucrose solutions, but with a marked increase in the magnitude of the pull-off force at equivalent slow velocities. Again, the observed increase in the pull-off force with the addition of sucrose observed here cannot be attributed to hydrodynamic effects because of the slow velocities involved, and the fact that the pull-off increases at slower velocities. However, decrease in interfacial tension from the sucrose also leads to an increased deformability of drops and may lead to both an increase in film thickness during the interaction and an increase in the interaction area. Caution must therefore be taken in direct comparison of aqueous solutions and sucrose aqueous solutions. The increased film thickness in the sucrose system is likely to decrease the magnitude of the pull-off, whereas the increased interaction area and viscosity may both

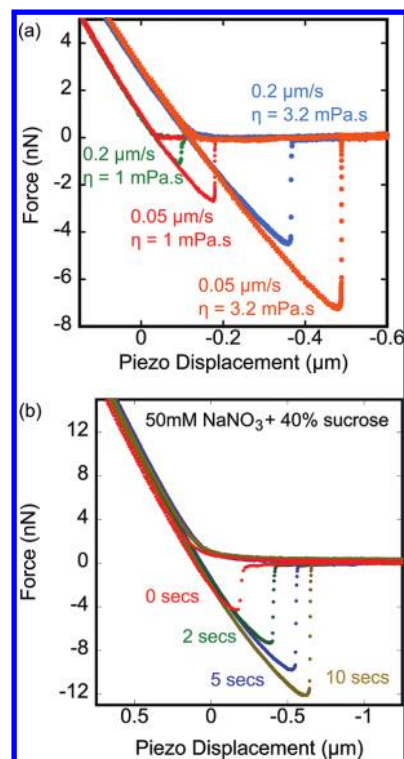


**Figure 8.** (a) Force as a function of piezo displacement for interactions between tetradecane drops of 70 and 43  $\mu\text{m}$  radii in 50 mM  $\text{NaNO}_3$  aqueous solution ( $\eta = 1.0$  mPa s), and between tetradecane drops of 38 and 75  $\mu\text{m}$  radii in 50 mM  $\text{NaNO}_3$  30% sucrose aqueous solution ( $\eta = 3.2$  mPa s). (b) Force as a function of piezo displacement for interactions between tetradecane drops of 38 and 75  $\mu\text{m}$  radii in 50 mM  $\text{NaNO}_3$  40% sucrose aqueous solution (6.2 mPa s) at 2  $\mu\text{m/s}$  collision velocity and dwell time at maximum force as indicated. Viscosities provided at laboratory conditions of force measurements.<sup>37</sup>

contribute to the observed increase in the magnitude of the pull-off effect observed.

The notion that the time for which the drops are in close contact is an important factor in determining the depth of the pull-off minimum is explored further in Figure 8b where drops are held at close separation by using the “dwell” function of the AFM. The selection of dwell time allows the time at which the drops are held at the point of greatest piezo translation from the starting piezo position (generally corresponding to the maximum force) before retraction. When no dwell is programmed (as for all data presented here thus far), the piezo will extend over the specified distance and turn around to reverse direction of motion with no pause. In Figure 8b, the increase in dwell, and hence the time over which the drops are in close contact, is demonstrated to systematically increase the magnitude of the pull-off force on retract.

The pull-off phenomenon on retract has been observed with a range of purified oil-drop types, including pure hexadecane, 3:1 mixtures of tetradecane and hexadecane, pure tetradecane, and octyl acetate. The results for the alkane systems, regardless of solubility, show that the behavior does not change markedly for a given salt species. Use of a more polar oil (octyl acetate) of greater aqueous solubility results in the onset of the pull-off interaction at lower salt concentration (10 mM), possibly connected with ion-specificity results reported for polar oils interacting with silica.<sup>32</sup> Thus, this behavior is observable for both sparingly soluble and slightly soluble oils.

## 4. DISCUSSION

Hydrodynamic interactions between tetradecane drops at 50 and 500 mM, where the velocity of drop approach is comparable to the rate of film drainage, show that forces can be predicted by the continuum theoretical model based on bulk viscosity in the thin film, and a DLVO disjoining pressure. A pull-off minimum force is observed on retract at slower velocities, where the time of the interaction is longer; however, the film thickness is at least that of the hydrodynamic case at 500 mM ( $\sim 2$  nm), where theoretical modeling accurately describes the force behavior. This suggests that there is some time-dependent phenomenon occurring in the thin film, supported by the observation that the magnitude of the pull-off force can be increased by reducing velocity (Figures 3b and 4), increasing piezo extension (Figure 4) or increasing dwell time (Figure 8b), all of which act to increase the time of interaction.

A conclusive physical picture of the origins of these observations remains elusive, although a range of speculative explanations for the experimental observations can be argued. A number of these have been assessed with the discussion here limited to a few clarifying points. Although the interaction appears qualitatively similar in nature to an adhesion force that has been observed in solid–solid contacts, the physical interaction is most likely very different as it is highly unlikely to involve direct drop–drop contact. The drop size is unchanged in instances where coalescence does not occur, and formation of a short-lived capillary oil bridge is unlikely as the curvature of such a configuration is highly unstable and would result in immediate coalescence.<sup>2</sup> The observation of constant drop size over the course of the interaction also suggests that Ostwald ripening does not occur to any significant extent. Indeed, Ostwald ripening is not expected given that the duration of the interaction is seconds and the low solubility of the oils requires days for any substantial effects of ripening to be observed.<sup>38</sup> A change in viscosity for thin films of  $\sim 2$  nm was not observed in dynamic interactions at 500 mM salt concentration that were accurately modeled with a constant viscosity. This suggests that viscosity is near that of the bulk fluid, even under confinement. The magnitude of the pull-off has been demonstrated to be anion-specific. There are a number of pathways for ions to effect colloidal interactions, including the varying affinity of ions for the interfacial region<sup>39,34,40</sup> and ion-effects on water molecule dipole alignments at interfaces.<sup>14,16,33</sup> However, given the inability to model data with an identifiable surface force or drainage phenomena, attempting to connect interfacial ion-behavior and the pull-off interaction observed in this study would be highly speculative.

## 5. CONCLUSIONS

This work shows accurate modeling of experimental drop–drop collisions at fast collision velocities, including prediction of coalescence behavior at a salt concentration of 500 mM. At slower velocities, continuum models appear to break down, when films thin to  $\sim 2$ – $7$  nm. An increase in time of drop–drop interaction, or drainage time, promotes a noncontinuum pull-off force on drop–drop retract in aqueous solutions. An increase is seen in the minimum force prior to pull-off with particular anions. The pull-off interaction may support other observations of anion-dependent interfacial water structuring effects at oil–water interfaces,<sup>14,33</sup> with the possibility that such

structuring provides an additional resistance to drainage. However, without an accurate knowledge of film thickness, a proven model of surface forces, including the dynamic behavior of ions in this confined region, deviations from bulk fluid flow cannot be quantified. Understanding of the time-dependent pull-off force may evolve with further theoretical and experimental studies of the molecular structure of confined oil–water interfacial regions, in particular the interplay and kinetics of ion and water molecule behavior in the final stages of film drainage.

## ■ AUTHOR INFORMATION

### Corresponding Author

\*E-mail: rrd@unimelb.edu.au.

### Notes

The authors declare no competing financial interest.

## ■ ACKNOWLEDGMENTS

X. S. Tang and S. O'Shea are thanked for preparing the cantilevers used. The ARC is thanked for financial support, and the Particulate Fluids Processing Centre provided infrastructure support for the project.

## ■ REFERENCES

- (1) Grigoriev, D. O.; Miller, R. *Curr. Opin. Colloid Interface Sci.* **2009**, *14*, 48.
- (2) Gunes, D. Z.; Clain, X.; Breton, O.; Mayor, G.; Burbidge, A. S. *J. Colloid Interface Sci.* **2010**, *343*, 79.
- (3) Vakarelski, I. U.; Manica, R.; Tang, X. S.; O'Shea, S. J.; Stevens, G. W.; Grieser, F.; Dagastine, R. R.; Chan, D. Y. C. *Proc. Natl. Acad. Sci. U.S.A.* **2010**, *107*, 11177.
- (4) Dagastine, R. R.; Manica, R.; Carnie, S. L.; Chan, D. Y. C.; Stevens, G. W.; Grieser, F. *Science* **2006**, *313*, 210.
- (5) Carnie, S. L.; Chan, D. Y. C.; Lewis, C.; Manica, R.; Dagastine, R. R. *Langmuir* **2005**, *21*, 2912.
- (6) Webber, G. B.; Edwards, S. A.; Stevens, G. W.; Grieser, F.; Dagastine, R. R.; Chan, D. Y. C. *Soft Matter* **2008**, *4*, 1270.
- (7) Henry, C. L.; Craig, V. S. *J. Phys. Chem. Chem. Phys.* **2009**, *11*, 9514.
- (8) Honig, C. D. F.; Ducker, W. A. *J. Phys. Chem. C* **2007**, *111*, 16300.
- (9) Honig, C. D. F.; Ducker, W. A. *Phys. Rev. Lett.* **2007**, *98*, 028305/1–028305/4.
- (10) Khan, S. H.; Matei, G.; Patil, S.; Hoffmann, P. M. *Phys. Rev. Lett.* **2010**, *105*, 106101.
- (11) Raviv, U.; Perkin, S.; Laurat, P.; Klein, J. *Langmuir* **2004**, *20*, 5322.
- (12) Jena, K. C.; Hore, D. K. *J. Phys. Chem. C* **2009**, *113*, 15364.
- (13) Brown, M. G.; Walker, D. S.; Raymond, E. A.; Richmond, G. L. *J. Phys. Chem. B* **2003**, *107*, 237.
- (14) McFearn, C. L.; Richmond, G. L. *J. Phys. Chem. C* **2009**, *113*, 21162.
- (15) Ninham, B. W.; Yaminsky, V. *Langmuir* **1997**, *13*, 2097.
- (16) Collins, K. D.; Washabaugh, M. W. *Q. Rev. Biophys.* **1985**, *18*, 323.
- (17) Perkin, S.; Goldberg, R.; Chai, L.; Kampf, N.; Klein, J. *Faraday Discuss.* **2009**, *141*, 399.
- (18) Beattie, J. K.; Djerdjev, A. M.; Franks, G. V.; Warr, G. G. *J. Phys. Chem. B* **2005**, *109*, 15675.
- (19) Lockie, H. E.; Manica, R.; Stevens, G. W.; Grieser, F.; Chan, D. Y. C.; Dagastine, R. R. *Langmuir* **2011**, *27*, 2676.
- (20) Gray-Weale, A.; Beattie, J. K. *Phys. Chem. Chem. Phys.* **2009**, *11*, 10994.
- (21) Tabor, R. F.; Chan, D. Y. C.; Grieser, F.; Dagastine, R. R. *Angew. Chem., Int. Ed.* **2011**, *50*, 3454.

- (22) Manor, O.; Vakarelski, I. U.; Tang, X.; O'Shea, S. J.; Stevens, G. W.; Grieser, F.; Dagastine, R. R.; Chan, D. Y. C. *Phys. Rev. Lett.* **2008**, *101*, 024501.
- (23) Hutter, J. L.; Bechhoefer, J. *Rev. Sci. Instrum.* **1993**, *64*, 1868.
- (24) Dagastine, R. R.; Webber, G. B.; Manica, R.; Stevens, G. W.; Grieser, F.; Chan, D. Y. C. *Langmuir* **2010**, *26*, 11921.
- (25) Tabor, R. F.; Lockie, H.; Mair, D.; Manica, R.; Chan, D. Y. C.; Grieser, F.; Dagastine, R. R. *J. Phys. Chem. Lett.* **2011**, *2*, 961.
- (26) Dagastine, R. R.; White, L. R. *J. Colloid Interface Sci.* **2002**, *247*, 310.
- (27) Chan, D. Y. C.; Dagastine, R. R.; White, L. R. *J. Colloid Interface Sci.* **2001**, *236*, 141.
- (28) Dagastine, R. R.; Chau, T. T.; Chan, D. Y. C.; Stevens, G. W.; Grieser, F. *World Congr. Chem. Eng., 7th* **2005**, 86500.
- (29) Israelachvili, J. N. *Intermolecular and Surface Forces*; Academic Press: San Diego, CA, 1991.
- (30) Bhatt, D.; Newman, J.; Radke, C. J. *Langmuir* **2001**, *17*, 116.
- (31) Tabor, R. F.; Chan, D. Y. C.; Grieser, F.; Dagastine, R. R. *J. Phys. Chem. Lett.* **2011**, *2*, 434.
- (32) Dagastine, R. R.; Chau, T. T.; Chan, D. Y. C.; Stevens, G. W.; Grieser, F. *Faraday Discuss.* **2005**, *129*, 111.
- (33) Shamay, E. S.; Richmond, G. L. *J. Phys. Chem. C* **2011**, *114*, 12590.
- (34) Levin, Y.; dos Santos, A. P.; Diehl, A. *Phys. Rev. Lett.* **2009**, *103*, 257802.
- (35) Bremond, N.; Thiam, A. R.; Bibette, J. *Phys. Rev. Lett.* **2008**, *100*, 4.
- (36) Chan, D. Y. C.; Klaseboer, E.; Manica, R. *Soft Matter* **2009**, *5*, 2858.
- (37) Haynes, W. M.; Lide, D. R. *CRC Handbook of Chemistry and Physics*, 91st ed.; CRC Press: New York, 2011.
- (38) Taylor, P. *Adv. Colloid Interface Sci.* **1998**, *75*, 107.
- (39) Jungwirth, P.; Tobias, D. J. *Chem. Rev.* **2006**, *106*, 1259.
- (40) Borukhov, I.; Andelman, D.; Orland, H. *Electrochim. Acta* **2000**, *46*, 221.